

INSTRUCTTA: Instruction-Tuned Targeted Attack for Large Vision-Language Models

Xunguang Wang, Zhenlan Ji, Pingchuan Ma, Zongjie Li, Shuai Wang
The Hong Kong University of Science and Technology
Hong Kong, China

{xwanghm, zjiae, pmaab, zligo, shuaiw}@cse.ust.hk

Abstract

Large vision-language models (LVLMs) have demonstrated their incredible capability in image understanding and response generation. However, this rich visual interaction also makes LVLMs vulnerable to adversarial examples. In this paper, we formulate a novel and practical gray-box attack scenario that the adversary can only access the visual encoder of the victim LVLM, without the knowledge of its prompts (which are often proprietary for service providers and not publicly available) and its underlying large language model (LLM). This practical setting poses challenges to the cross-prompt and cross-model transferability of targeted adversarial attack, which aims to confuse the LVLM to output a response that is semantically similar to the attacker’s chosen target text. To this end, we propose an instruction-tuned targeted attack (dubbed INSTRUCTTA) to deliver the targeted adversarial attack on LVLMs with high transferability. Initially, we utilize a public text-to-image generative model to “reverse” the target response into a target image, and employ GPT-4 to infer a reasonable instruction p' from the target response. We then form a local surrogate model (sharing the same visual encoder with the victim LVLM) to extract instruction-aware features of an adversarial image example and the target image, and minimize the distance between these two features to optimize the adversarial example. To further improve the transferability, we augment the instruction p' with instructions paraphrased from an LLM. Extensive experiments demonstrate the superiority of our proposed method in targeted attack performance and transferability.

1. Introduction

Large vision-language models (LVLMs) have achieved great success in text-to-image generation [35], image captioning [7] and visual question-answering [25], due to the colossal increase of training data and model parameters.

Benefiting from the strong comprehension of large language models (LLMs), recent LVLMs [12, 25, 27, 48] on top of LLMs have demonstrated a superior capability in solving complex tasks than that of small vision-language models. It is noted that GPT-4 [32] supports visual inputs and perform human-like conversations in various complicated scenarios.

However, recent studies [3, 15, 36, 46] exposed that LLMs with visual structures could be easily fooled by adversarial examples (AEs) crafted via adding imperceptible perturbations to benign images. In particular, targeted attack with malicious goal raises more serious safety concerns to LVLMs and downstream applications. For example, targeted adversarial examples could jailbreak LVLMs to explain the bomb-making process or trick medical diagnostic models into generating reports of specific diseases for insurance. It is thus demanding to comprehensively study adversarial attacks on LVLMs to address these security threats before security breaches happen.

This paper focuses on the targeted attack on LVLMs, where the adversary aims to generate an adversarial image that misleads the LVLM to respond with a specific target text, despite varying instructions the LVLM may use. We target a practical gray-box setting, where the adversary can only access the visual encoder of the LVLM without any knowledge of the LLM and instructions leveraged by the LVLM.¹ While de facto LVLMs often leverage standard visual encoders that are publicly known, the employed instructions are often proprietary for service providers and not publicly available. This practical assumption brings some key challenges: (1) The attacker cannot easily gain the instruction-aware features from the accessed visual encoder to launch exact targeted attacks due to a lack of instructions. (2) Cross-model and cross-instruction transferability places new demands on the targeted attack, since the target LVLM may have distinct LLM backends and use varying (unknown) instructions.

¹To clarify, in this paper, we use the term “instruction” and “prompt” interchangeably.

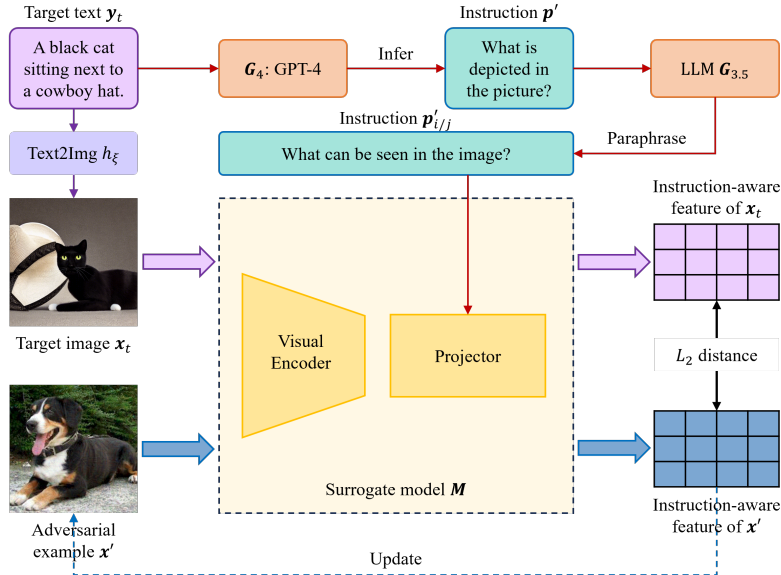


Figure 1. The framework of our instruction-tuned targeted attack (INSTRUCTTA). Given a target text y_t , we first transform it into the target image x_t with a text-to-image model h_ξ . Simultaneously, GPT-4 infers a reasonable instruction p' . When feeding the augmented instruction p'_i and p'_j rephrased by an LLM $G_{3.5}$, the surrogate model M extracts instruction-aware features of the AE x' and x_t , respectively. Finally, we minimize the L_2 distance between these two features to optimize the AE x' . Notably, the instruction $p'_{i/j}$ is updated on-the-fly during the optimization of the adversarial sample.

To overcome these challenges, this paper proposes an instruction-tuned targeted attack (INSTRUCTTA) for LVLMs with high attack transferability. As depicted in Fig. 1, we first employ GPT-4 [32] to infer an instruction p' in line with the attacker-decided response, and also generate a target image for the target response using a text-to-image generative model. Subsequently, we take both images and instructions as inputs to a local surrogate model to extract informative features tailored to the target response. INSTRUCTTA then minimizes the feature distance between the adversarial image example and the target image. Moreover, INSTRUCTTA rephrases p' into a set of instructions with close semantics, and leverages them to effectively improve the transferability of generated adversarial samples. Our main contributions are outlined as follows:

- This paper explores the attack vector of LVLMs under a practical yet unexplored gray-box setting, *i.e.*, the adversary only has the rights to access the visual encoder in LVLMs, excluding the LLM and instructions.
- We propose an effective targeted attack, INSTRUCTTA. It cleverly leverages text-to-image models and LLMs to infer reasonable target images and instructions, respectively, and augments the transferability of adversarial samples with instruction-tuning paradigms.
- Extensive experiments demonstrate that INSTRUCTTA can achieve better targeted attack performance and transferability than intuitive baselines. We also discuss mitigations and ethics considerations of INSTRUCTTA.

2. Related Work

LVLMs. Benefiting from the powerful capabilities of LLMs in answering diverse and complex questions [31], LVLMs [46] have demonstrated remarkable performance on a variety of multi-modal tasks, *e.g.*, image captioning, visual question-answering, natural language visual reasoning and visual dialog. To bridge the image-text modality gap, BLIP-2 [25] proposes the Q-Former to extract visual features into the frozen OPT [45] or FlanT5 [11]. MiniGPT-4 [48] employs the identical pretrained ViT [16] and Q-Former as BLIP-2, but uses the more powerful Vicuna [10] to serve as the base LLM for text generation. InstructBLIP [12] introduces an instruction-aware Q-Former to extract the most task-relevant visual representations. LLaVA [27] bridges a pre-trained visual encoder with LLaMA, and fine-tunes them with question-image-answer paired data generated by GPT-4.

Adversarial Attacks. Although adversarial attacks are now being developed in a variety of modalities and tasks, the earliest and most extensive research occurred in the field of image classification [4, 37]. In this case, the goal of adversarial attack is often to fool a well-trained visual classifier by crafted adversarial images. Based on their purpose, we divide adversarial attacks into *targeted attacks* and *non-targeted attacks* [2]. Targeted attacks aim to confuse the model to recognize the adversarial example as a target label, whereas non-targeted attacks only ensure that the model

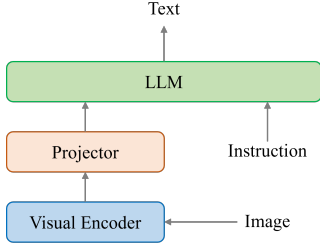


Figure 2. The architecture of LVLM.

make wrong predictions, not caring about the output error category. Moreover, according to the information of the attacked model exposed to the adversary, adversarial attacks can be grouped into white-box attack and black-box attack. The white-box attacks can obtain the whole parameters and structure of the target model. Thus, they generally optimize adversarial perturbations with gradients of loss *w.r.t* inputs, *e.g.*, FGSM [19], I-FGSM [22], C&W[5] and PGD [30]. In contrast, only the input and output of the attacked model can be captured by black-box attack, which is more challenging and practical than white-box one. One solution is to estimate the gradient or search for successful perturbations by directly querying the target model multiple times, *e.g.*, ZOO [8] and NES attack [21]. Another way is to implement *transfer attacks* by constructing adversarial samples from substitute models, *e.g.*, SBA [33] and ensemble-based approaches [14, 18, 20, 28].

Besides image classification, researchers have extended adversarial attacks to vision-language models or tasks [6, 23, 26, 29, 38–41, 43, 46, 47]. Recently, investigating adversarial robustness on vision-language pre-training (VLP) models [29, 39, 43] has aroused much attention. Zhang *et al.* [43] proposed Co-Attack for VLP models, which collaboratively combines the image and the text perturbations. SGA [29] improved the adversarial transferability across different VLP models by breaking the set-level cross-modal alignment.

AEs on LVLMs. Currently, there are some pioneering and contemporaneous works of targeted attacks on LVLMs. On one hand, some works aim to mislead the LVLMs to output specific words. For example, Bailey *et al.* [3] forces the LVLM to respond with the target string in a white-box setting. Dong *et al.* [15] present text description attack to mislead the black-box Bard [1] to output targeted responses, which maximize the log-likelihood of the substitute LVLMs to predict the target sentence. On the other hand, some works have been devoted to fooling LVLMs into outputting text with the same semantics as the target. For example, Zhao *et al.* [46] propose three feature matching methods (*i.e.*, MF-it, MF-ii and MF-tt) to launch targeted attack with given target text against LVLMs in black-box settings. Shayegani *et al.* [36] also align the adversarial im-

age and target images in the embedding space for LVLM jailbreak. Different from [46], we focus on the gray-box setting instead of the black-box setting, and further improve the attack transferability under the guidance of inferred and rephrased instructions. While [36] also accesses visual encoders in LVLMs for jailbreak, our work highlights the capability to implement generic targeted attacks even without knowing the target LVLM’s instructions.

3. Method

3.1. Problem Formulation

LVLM. Given an image x and a text instruction p as inputs, the LVLM F outputs an answer y . Formally,

$$y = F_{\theta}(x, p), \quad (1)$$

where F_{θ} denotes the LVLM parameterized by θ . Typically, the LVLM [12, 25, 27, 48] projects the extracted visual features into the word embedding space and then feeds them to its underlying LLM. Hence, LVLM consists of a pre-trained visual encoder, a projector and a well-trained LLM, as shown in 2.

Adversarial Objective. In image-grounded text generation, the goal of targeted attack is to construct adversarial examples, which could cause the output of the victim model to match a predefined targeted response. Under the L_{∞} norm constraint, the objective of a targeted attack can be formulated as follows:

$$\begin{aligned} \Delta(x, y_t) &:= \max_{x'} S(F(x', p), y_t), \\ \text{s.t. } &\|x' - x\|_{\infty} \leq \epsilon, \end{aligned} \quad (2)$$

where x is a given benign image sample, x' represents the adversarial example of x , and y_t denotes the predefined target text. ϵ is the budget of controlling adversarial perturbations, and p denotes the instructions used by the target LVLM (p is unknown to attackers; see § 3.2). $S(\cdot, \cdot)$ is a metric depicting the semantic similarity between two input sentences. This way, Eqn. 2 ensures that the response of the adversarial example shall retain the same meaning as the target text y_t .

3.2. Targeted Attack with Instruction Tuning

Assumption. In this paper, we consider a practical gray-box setting, where the adversary only knows the visual encoder used in the attacked model, excluding LLMs and instructions of the victim LVLM. That is, the adversary is agnostic to p . Instead, we assume that attackers know the usage domain of the target LVLM, *e.g.*, CT image diagnosis; considering F is often hosted as a task-specific service, attackers can easily obtain this information. Accordingly, attackers can locally prepare instructions p' which are commonly used in the target domain (see below for details). We also

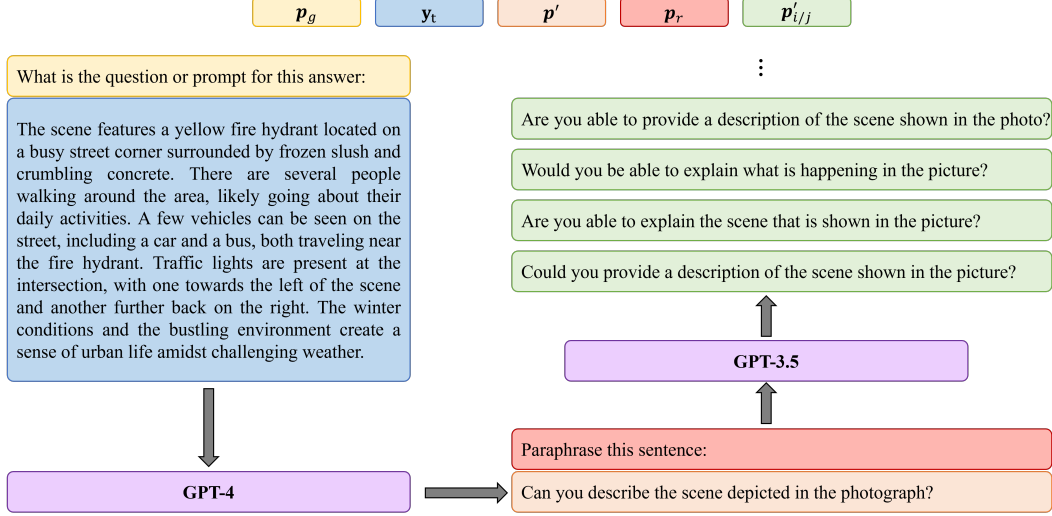


Figure 3. An example of rephrasing an instruction. Given the target response \mathbf{y}_t , GPT-4 infers an instruction, i.e., “Can you describe the scene depicted in the photograph?”. The real instruction assigned to this target text is “Explain the visual content of the image in great detail.”

Algorithm 1 INSTRUCTTA

Input: a benign image \mathbf{x} , a target text \mathbf{y}_t , a text-to-image generative model h_ξ , a surrogate model M , a VLP model with the visual encoder f and text encoder g , ChatGPT $G_{3.5}$, GPT-4 G_4 , custom prompts \mathbf{p}_g and \mathbf{p}_r , step size η , perturbation budget ϵ , attack iterations T

- 1: **Initialize:** $\mathbf{x}' = \mathbf{x}$, $\mathbf{x}_t = h_\xi(\mathbf{y}_t)$,
 $\mathbf{p}' = G_4(\mathbf{p}_g \mathbf{y}_t)$ // Eqn. (3)
- 2: **for** $iter = 1 \dots T$ **do**
- 3: $\mathbf{p}'_i \leftarrow G_{3.5}(\mathbf{p}_r \mathbf{p}')$
- 4: $\mathbf{p}'_j \leftarrow G_{3.5}(\mathbf{p}_r \mathbf{p}'_i)$
- 5: $\mathbf{x}' = \mathcal{S}_\epsilon(\mathbf{x}' - \eta \cdot \text{sign}(\Delta_{\mathbf{x}' \mathcal{L}}))$ // PGD
- 6: **end for**

Output: adversarial example \mathbf{x}'

assume that before attack, attackers can form a local surrogate model with the same visual encoder as that of the victim model.

Inferring Instructions. We first locally infer the possible instructions \mathbf{p}' for the target text \mathbf{y}_t by using GPT-4 [32]. Formally,

$$\mathbf{p}' = G_4(\mathbf{p}_g \mathbf{y}_t), \quad (3)$$

where G_4 denotes the language-only GPT-4, and \mathbf{p}' represents an instruction generated by G_4 . The above action denotes that we feed an instruction \mathbf{p}_g concatenated with the target response text \mathbf{y}_t to the GPT-4. In the experiment, we set \mathbf{p}_g to a straightforward prompt “What is the question or prompt for this answer:”.

Forming Surrogate Models. Once the instructions have been inferred, the surrogate model uses a projector to trans-

form the features from the visual encoder into instruction-aware features. Thus, the surrogate model comprises two modules: the visual encoder from the victim model and the pre-trained projector (e.g., Q-Former [25]). The projector maps global visual features into informative features tailored to given instructions.

Generating Adversarial Examples. We then extract the instruction-aware visual features most conducive to the task by inputting both images and the generated instructions to the surrogate model. For the targeted attack, a simple solution is to align the adversarial example to the target text in the feature space of the substitute model. Given that the surrogate model only extracts visual features, it fails to build target embedding for the target text. An alternative approach is to transform the target text into the target image through text-to-image generative models (e.g., Stable Diffusion [35]). Hence, we reduce the embedding distance between the adversarial example and the target image \mathbf{x}_t for the targeted attack as:

$$\min_{\mathbf{x}'} \|M(\mathbf{x}', \mathbf{p}') - M(h_\xi(\mathbf{y}_t), \mathbf{p}')\|_2^2, \quad \text{s.t. } \|\mathbf{x}' - \mathbf{x}\|_\infty \leq \epsilon \quad (4)$$

where $M(\cdot, \cdot)$ denotes the substitute model, h_ξ is a public generative model ($\mathbf{x}_t = h_\xi(\mathbf{y}_t)$), and \mathbf{x}' indicates the adversarial sample of \mathbf{x} .

Augmenting Transferability. Our tentative exploration shows that AEs generated by Eqn. 4, although manifesting reasonable attackability, are often less transferable to the wide range of possible instructions in the wild. Thus, to improve the transferability and robustness of the generated adversarial examples, we use ChatGPT (i.e., GPT-3.5) to rephrase the inferred \mathbf{p}' as augmentation. The paraphrase

prompt template fed into the ChatGPT is “*Paraphrase this sentence:*”. This way, Eqn. 4 can be rewritten as

$$\min_{\mathbf{x}'} \mathcal{J}_{ins} = \mathbb{E}_{\mathbf{p}'_i, \mathbf{p}'_j} \|M(\mathbf{x}', \mathbf{p}'_i) - M(h_\xi(\mathbf{y}_t), \mathbf{p}'_j)\|_2^2, \quad (5)$$

$$\text{s.t. } \|\mathbf{x}' - \mathbf{x}\|_\infty \leq \epsilon,$$

where \mathbf{p}'_i and \mathbf{p}'_j are augmented instructions from \mathbf{p}' . Both of them are generated by ChatGPT, *i.e.*, $\mathbf{p}'_i = G_{3.5}(\mathbf{p}_r \mathbf{p}')$, $\mathbf{p}'_j = G_{3.5}(\mathbf{p}_r \mathbf{p}')$, where $G_{3.5}$ represents ChatGPT and \mathbf{p}_r denotes the aforementioned rephrasing template. As illustrated in Fig. 3, ChatGPT is generally effective to rephrase a seed instruction \mathbf{p}' into a set of semantically-correlated instructions.

3.3. Dual Targeted Attack & Optimization

With the aforementioned steps, we form following dual targeted attack framework:

$$\arg \min_{\mathbf{x}'} \mathcal{L} = \mathcal{J}_{ins} - \mathcal{J}_{mf}, \quad \text{s.t. } \|\mathbf{x}' - \mathbf{x}\|_\infty \leq \epsilon, \quad (6)$$

where \mathcal{J}_{mf} is the objective of MF-it or MF-ii, following [46]. MF-it and MF-ii achieve transfer targeted attack via matching the embeddings of the adversarial example and the target response. For MF-it, its objective is defined as

$$\mathcal{J}_{mf} = [f(\mathbf{x}')]^T g(\mathbf{y}_t), \quad (7)$$

where $f(\cdot)$ and $g(\cdot)$ are the paired visual encoder and text encoder of an align-based VLP model (*e.g.*, CLIP [34], ALBEF [24], Open-CLIP [9], and EVA-CLIP [17]), respectively. For MF-ii, we have

$$\mathcal{J}_{mf} = [f(\mathbf{x}')]^T f(h_\xi(\mathbf{y}_t)). \quad (8)$$

Notably, Eqn. 6 with MF-it is marked INSTRUCTTA-MF-it, and Eqn. 6 with MF-ii is marked INSTRUCTTA-MF-ii.

When optimizing adversarial samples following Eqn. 6, this paper adopts PGD to update \mathbf{x}' with T iterations as below,

$$\mathbf{x}'_T = \mathcal{S}_\epsilon(\mathbf{x}'_{T-1} - \eta \cdot \text{sign}(\Delta_{\mathbf{x}'_{T-1}} \mathcal{L})), \quad \mathbf{x}'_0 = \mathbf{x}, \quad (9)$$

where η denotes step size, and \mathcal{S}_ϵ clips \mathbf{x}' into the ϵ -ball [30] of \mathbf{x} .

In Algorithm 1, we outline the whole pipeline of INSTRUCTTA. Initially, once decided an adversarial target text \mathbf{y}_t , we use the text-to-image model h_ξ and GPT-4 to “reverse” a target image \mathbf{x}_t and produce the reference instruction \mathbf{p}' , respectively. In each iteration, we augment the inferred instruction \mathbf{p}' with ChatGPT firstly. Then, we update the adversarial example with PGD over Eqn. 6. Until the end of T step iterations, the final adversarial sample is obtained and used for attacking remote LVLMS.

4. Experiments

This section presents the experimental results of the proposed INSTRUCTTA on multiple victim LVLMS. We introduce the evaluation setup in § 4.1, and then present the results in § 4.2 followed by ablation study in § 4.3 and discussion in § 4.4.

4.1. Evaluation Setup

Datasets. The ImageNet-1K [13] comprises 3 subsets, including training, validation and test sets. We randomly select 1,000 images from the validation set to serve as the benign samples (\mathbf{x}) for the attack. Correspondingly, we sample 1,000 instruction-answer pairs from LLaVA-Instruct-150K [27] as tested instructions and target texts, respectively, since LLaVA-Instruct-150K is a set of multimodal instruction-following data generated by GPT-4. In addition, we use Stable Diffusion (h_ξ) to generate target images from the target texts, following [46].

Protocols. Following [46], we adopt CLIP-score (\uparrow) to evaluate the targeted attack performance, which calculates the semantic similarity between the generated response of victim LVLMS and the target text using CLIP text encoders. Additionally, we record the number of successful attacks by using GPT-4 to determine whether two texts have the same meaning. The prompt in this operation is as follows:

Determine whether these two texts describe the same objects or things, you only need to answer yes or no:

1. \mathbf{y}'
2. \mathbf{y}_t

where \mathbf{y}' denotes the output response of the adversarial example on victim model, and \mathbf{y}_t is the target response.

Baselines. This paper provides evaluations on three victim LVLMS, including BLIP-2 [25], InstructBLIP [12] and MiniGPT-4 [48]. In detail, we select flan-t5-xxl², vicuna-7b-v1.1³ and vicuna-v0-13b⁴ as LLMs for BLIP-2, InstructBLIP and MiniGPT-4, respectively. Their visual encoders are all ViT-G/14 [42] borrowed from EVA-CLIP [17]. To evaluate the targeted attack performance, INSTRUCTTA is compared with existing baselines, *i.e.*, MF-it and MF-ii. They can choose CLIP (ViT-B/32) [34] or the EVA-CLIP (ViT-G/14) as surrogate models for targeted attacks.

Implementation Details. All images are resized to 224 × 224 before feeding in substitute models and LVLMS. For INSTRUCTTA, we choose the visual encoder and Q-Former from InstructBLIP as the surrogate model. For PGD, η and T are set to 1 and 100, respectively. The maximum perturbation magnitude ϵ is set to 8. We implement all the evaluations using Pytorch 2.1.0 and run them on a single NVIDIA RTX A6000 GPU (48G).

²<https://huggingface.co/google/flan-t5-xxl>

³<https://huggingface.co/lmsys/vicuna-7b-v1.1>

⁴<https://huggingface.co/Vision-CAIR/vicuna>

Table 1. **Targeted attacks against victim LVLMs.** A total of 1,000 clean images denoted as x are sampled from the ImageNet-1K [13] validation set. For each of these benign images, a targeted text y_t and a prompt p are randomly assigned from LLaVA-Instruct-150K [27]. Our analysis involves the computation of the CLIP score (\uparrow) [34, 46] between the target texts and the generated responses of AEs on attacked LVLMs, which was performed using several CLIP text encoders and their ensemble. We also report the No. of successful attacks within 1,000 adversarial samples, determined by GPT-4. CLIP and EVA-CLIP in parentheses indicate that they are used as surrogate models for transfer attack.

VLVM	Attack method	Text encoder (pretrained) for evaluation						The No. of successes
		RN50	RN101	ViT-B/16	ViT-B/32	ViT-L/14	Ensemble	
BLIP-2	Clean image	0.296	0.427	0.342	0.354	0.171	0.318	4
	MF-it (CLIP) [46]	0.292	0.424	0.339	0.353	0.168	0.315	2
	MF-ii (CLIP) [46]	0.293	0.426	0.340	0.353	0.168	0.316	2
	MF-it (EVA-CLIP)	0.574	0.667	0.616	0.630	0.481	0.594	519
	MF-ii (EVA-CLIP)	0.573	0.661	0.616	0.627	0.484	0.592	514
	INSTRUCTTA-MF-it (ours)	0.604	0.691	0.644	0.656	0.515	0.622	652
	INSTRUCTTA-MF-ii (ours)	0.599	0.682	0.639	0.649	0.512	0.616	619
InstructBLIP	Clean image	0.392	0.557	0.420	0.421	0.312	0.420	0
	MF-it (CLIP) [46]	0.394	0.558	0.423	0.422	0.313	0.422	0
	MF-ii (CLIP) [46]	0.395	0.557	0.424	0.423	0.314	0.422	0
	MF-it (EVA-CLIP)	0.773	0.822	0.791	0.796	0.740	0.785	292
	MF-ii (EVA-CLIP)	0.761	0.813	0.780	0.783	0.727	0.773	259
	INSTRUCTTA-MF-it (ours)	0.810	0.849	0.826	0.830	0.784	0.820	383
	INSTRUCTTA-MF-ii (ours)	0.789	0.833	0.805	0.809	0.758	0.799	328
MiniGPT-4	Clean image	0.345	0.495	0.367	0.374	0.253	0.367	0
	MF-it [46]	0.341	0.493	0.364	0.369	0.251	0.364	0
	MF-ii [46]	0.340	0.492	0.363	0.369	0.249	0.362	2
	MF-it (EVA-CLIP)	0.650	0.726	0.664	0.676	0.593	0.662	259
	MF-ii (EVA-CLIP)	0.649	0.723	0.665	0.670	0.592	0.660	247
	INSTRUCTTA-MF-it (ours)	0.692	0.756	0.701	0.712	0.638	0.700	363
	INSTRUCTTA-MF-ii (ours)	0.680	0.748	0.692	0.701	0.627	0.690	325

4.2. Results

Targeted Attack Performance. As illustrated in Table 1, we transfer adversarial samples generated by different targeted attack methods to victim LVLMs and mislead them to produce target responses. For each adversarial example, when attacking a LVLm, the target text and the assigned instruction may be different from other adversarial examples, since we randomly selected 1000 pairs of target texts and instructions from LLaVA-Instruct-150K [27]. Subsequently, we evaluate the similarity between the generated response y' of the victim LVLm and the targeted text y_t by utilizing diverse forms of CLIP text encoders, where $y' = F(x', p)$. In addition, we count the number of successful targeted adversarial samples, as judged by GPT-4.

Table 1 reports the evaluation results of different targeted attack methods on BLIP-2, InstructBLIP and MiniGPT-4. We compare INSTRUCTTA with MF-it and MF-ii, which are the two recent attacks on LVLms. Overall, we observe that INSTRUCTTA consistently outperforms MF-it and MF-ii in terms of CLIP score and the number of successful attacks. In fact, it can be seen that MF-it and MF-ii with CLIP have almost the same results as the clean samples, indicating no targeted attack effect. We believe this is reasonable, because ViT-B/32 in CLIP shares a different visual encoder than that of the target LVLm. In contrast, MF-it (EVA-CLIP), MF-ii (EVA-CLIP) and our methods all no-

tably outperform the targeted attack results on clean samples because they share the same visual encoder as the victim model. Overall, we interpret these results justify the necessity of using the same visual encoder as the victim model.

More importantly, both INSTRUCTTA-MF-it and INSTRUCTTA-MF-ii are distinctly better than MF-it and MF-ii in terms of CLIP-score and the number of successful attacks. These phenomena demonstrate that our method can effectively improve the transferability of the targeted attack on LVLms. One reason is that we enhance the robustness of AEs to varying instructions. Another reason is that our dual attacks (INSTRUCTTA-MF-it/INSTRUCTTA-MF-ii) extracts informative features containing global and instruction-aware knowledges, benefiting to precise targeted attacks.

Table 2. Ablation study of the proposed method on BLIP-2. CLIP score [46] is computed by ensemble CLIP text encoders. Attack success rate is the ratio between the No. of attack successes and the total No. of samples.

Attack method	CLIP score (\uparrow)	Attack success rate (\uparrow)
INSTRUCTTA-MF-it	0.622	0.652
INSTRUCTTA-MF-ii	0.616	0.619
INSTRUCTTA	0.606	0.624
INSTRUCTTA-woG	0.571	0.448

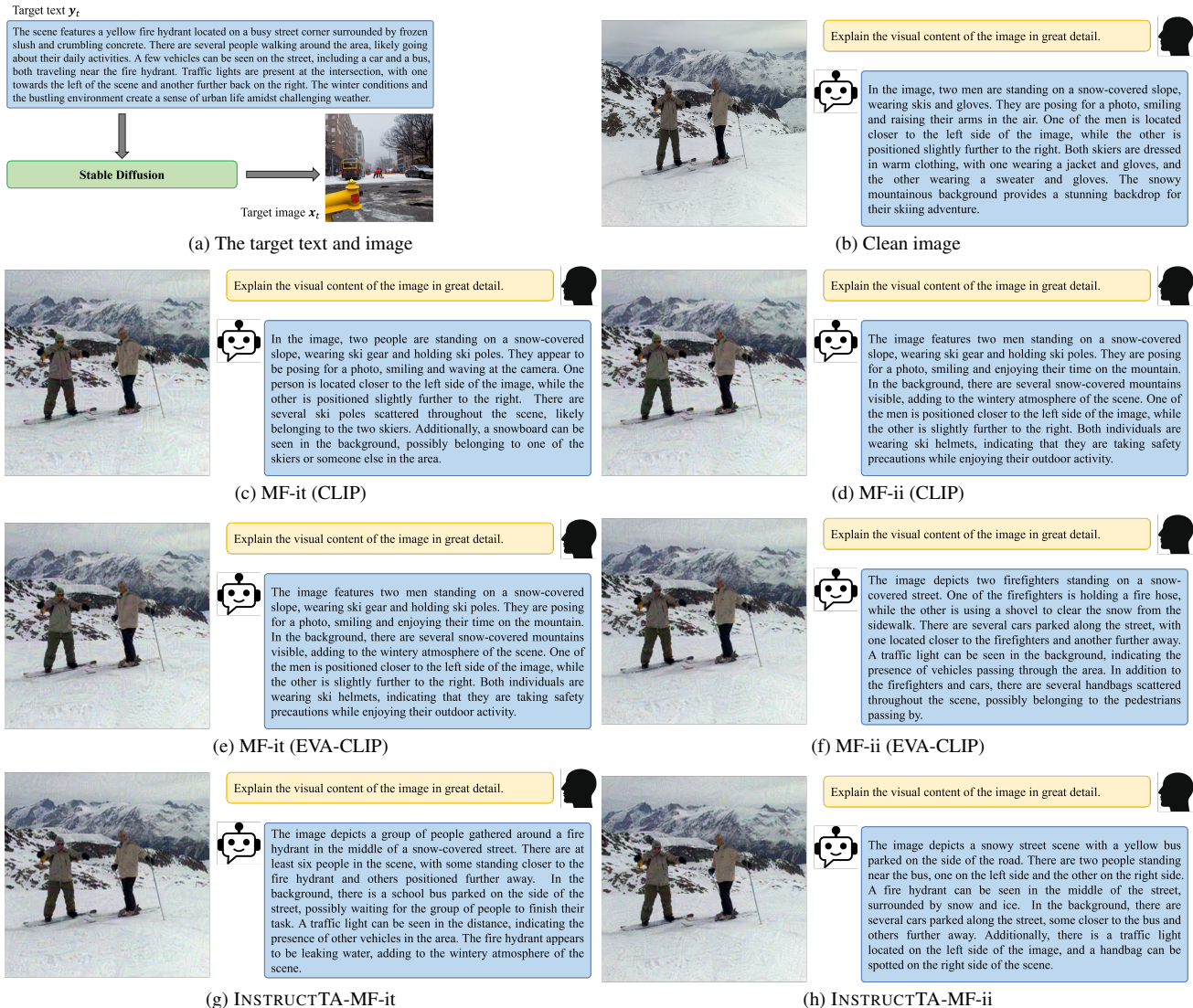


Figure 4. Visualization examples of various targeted attack methods on InstructBLIP. “Explain the visual content of the image in great detail.” is a real instruction.

Visualization Examples. Fig. 3 has displayed a sample inferred instruction and its sibling instructions rephrased by ChatGPT. It can be seen that the instructions inferred by GPT-4 are similar to the real instruction. The rephrased instructions are even more similar to the original sentence.

Moreover, we also provide some visual results of different attack methods on attacking InstructBLIP, as shown in Fig. 4. Overall, it can be observed that the generated responses of our methods are closer to the target texts.

4.3. Ablation Study

We also launched ablation study to explore the contribution of major components in the proposed method. At this step, we conducted experiments on BLIP-2 with two key

component ablated sequentially: 1) removing MF-it and MF-ii (denoted as INSTRUCTTA), and 2) launching optimization without CLIP embedding matching nor ChatGPT for paraphrase (in accordance with Eqn. 4; denoted as INSTRUCTTA-woG).

The results are reported in Table 2. It is observed that the performances degrade when one or more parts are removed. In particular, the INSTRUCTTA-woG setting exhibits a success rate downgrading of over 31% in comparison to the INSTRUCTTA-MF-it setting. Overall, we interpret the ablation study results as reasonable, illustrating that all the constituent components have been thoughtfully devised and exhibit congruity, culminating in an efficacious solution for the targeted attack.

Table 3. Targeted attack performance for multiple perturbation budget ϵ .

Budget ϵ	Text encoder (pretrained) for evaluation						Attack success rate
	RN50	RN101	ViT-B/16	ViT-B/32	ViT-L/14	Ensemble	
2	0.437	0.547	0.480	0.492	0.330	0.457	0.154
4	0.560	0.651	0.602	0.612	0.470	0.579	0.450
8	0.604	0.691	0.644	0.656	0.515	0.622	0.652
16	0.617	0.702	0.657	0.669	0.527	0.634	0.746
64	0.617	0.704	0.658	0.671	0.529	0.636	0.740

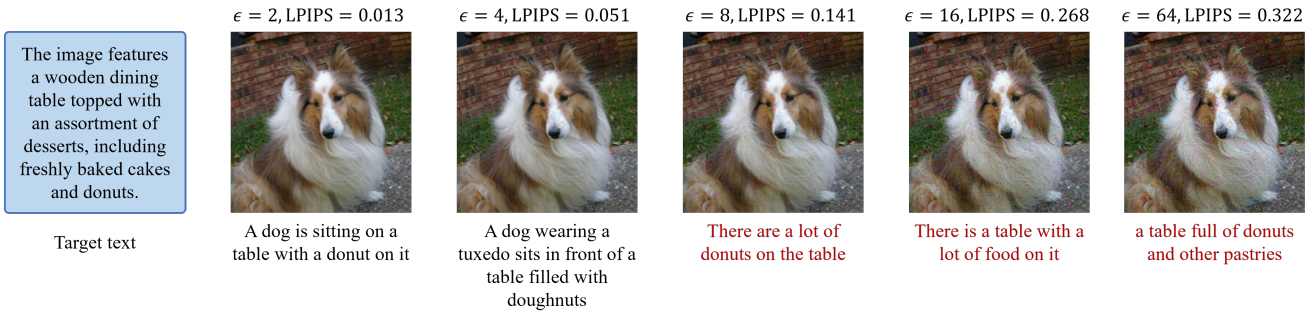


Figure 5. To explore the impact of varying ϵ values within the INSTRUCTTA-MF-it, we conducted experiments aiming to achieve different levels of perturbed images on BLIP-2, *i.e.*, referred to as the AE x' . Our findings indicate a degradation in the visual quality of x' , as quantified by the LPIPS [44] distance between the original image x and the adversarial image x' . Simultaneously, the effectiveness of targeted response generation reaches a saturation point. Consequently, it is crucial to establish an appropriate perturbation budget, such as $\epsilon = 8$, to effectively balance the image quality and the targeted attack performance.

4.4. Discussion

Effect of ϵ . To explore the effect of the perturbation magnitude ϵ on targeted attack performance, we study the attack results of INSTRUCTTA-MF-it toward BLIP-2 under various ϵ . The results are reported in Table 3. It is evident that with ϵ increasing, both CLIP scores and attack success rates rise, illustrating stronger attack performance. Nevertheless, it is seen that the attack performance becomes gradually saturated when ϵ is greater than 16. Moreover, as shown in Fig. 5, an overly large ϵ (*e.g.*, 16 and 64) has made the perturbation perceptible to naked eyes. Thus, we suggest to explore a proper ϵ for the targeted attack, *e.g.*, $\epsilon = 8$, such that the attack performance can be effectively improved while the perturbation is imperceptible.

Table 4. Average CLIP score (\uparrow) between different versions of instructions. Each type of instruction have 1,000 samples.

Instruction	Rephrased instruction $p'_{i/j}$	Real instruction p
Inferred instruction p'	0.942	0.883
Real instruction p	0.882	1.000

Assessment of Generated Instructions. To quantitatively evaluate the usability of the generated instructions, we collect a paraphrased instruction for each inferred instruction used in main experiment and provide average CLIP score values between them, as reported in Table 4. It is evident that there exists a high similarity score between the rephrased and the inferred instructions; moreover, the

rephrased and the inferred instructions both show high similarity with the real instructions. We interpret the results as encouraging, demonstrating the high quality of employed instructions.

5. Conclusion, Ethics, and Mitigation

Our work highlights the vulnerability of LVLMs to adversarial attacks under a practical, gray-box scenario. INSTRUCTTA delivers targeted attacks on LVLMs with high transferability, demonstrating the importance of instruction-based techniques and the fusion of visual and language information in boosting adversarial attacks. The aim of our work is to enhance the resilience of LVLMs. Ethically, since we discovered adversarial examples, we minimized harm by (1) avoiding any damage to real users and (2) disclosing the detailed attacking process and methods used to find them in this paper. Overall, we believe that the security of the LVLM ecosystem is best advanced by responsible researchers investigating these problems. Looking ahead, we envision the feasibility of launching various mitigation methods to improve the robustness of LVLMs against adversarial attacks. For instance, we can leverage the adversarial training framework [30] to train LVLMs with adversarial examples. We can also explore the possibility of incorporating adversarial training into the pre-training stage of LVLMs or their visual encoders. Moreover, we can also explore detecting adversarial examples by leveraging the discrepancy between the instruction-aware features of the adversarial examples and the original images.

References

- [1] Google bard, 2023. [3](#)
- [2] Naveed Akhtar and Ajmal Mian. Threat of adversarial attacks on deep learning in computer vision: A survey. *IEEE Access*, 6:14410–14430, 2018. [2](#)
- [3] Luke Bailey, Euan Ong, Stuart Russell, and Scott Emmons. Image hijacking: Adversarial images can control generative models at runtime. *arXiv preprint arXiv:2309.00236*, 2023. [1, 3](#)
- [4] Battista Biggio, Igino Corona, Davide Maiorca, Blaine Nelson, Nedin Šrđić, Pavel Laskov, Giorgio Giacinto, and Fabio Roli. Evasion attacks against machine learning at test time. In *Machine Learning and Knowledge Discovery in Databases*, pages 387–402, Berlin, Heidelberg, 2013. Springer Berlin Heidelberg. [2](#)
- [5] Nicholas Carlini and David Wagner. Towards evaluating the robustness of neural networks. In *IEEE Symposium on Security and Privacy*, pages 39–57, San Jose, CA, USA, 2017. IEEE. [3](#)
- [6] Hongge Chen, Huan Zhang, Pin-Yu Chen, Jinfeng Yi, and Cho-Jui Hsieh. Attacking visual language grounding with adversarial examples: A case study on neural image captioning. In *ACL*, 2018. [3](#)
- [7] Jun Chen, Han Guo, Kai Yi, Boyang Li, and Mohamed Elhoseiny. Visualgpt: Data-efficient adaptation of pretrained language models for image captioning. In *CVPR*, pages 18030–18040, 2022. [1](#)
- [8] Pin-Yu Chen, Huan Zhang, Yash Sharma, Jinfeng Yi, and Cho-Jui Hsieh. Zoo: Zeroth order optimization based black-box attacks to deep neural networks without training substitute models. In *ACM Workshop on Artificial Intelligence and Security*, pages 15–26, New York, NY, USA, 2017. Association for Computing Machinery. [3](#)
- [9] Mehdi Cherti, Romain Beaumont, Ross Wightman, Mitchell Wortsman, Gabriel Ilharco, Cade Gordon, Christoph Schuhmann, Ludwig Schmidt, and Jenia Jitsev. Reproducible scaling laws for contrastive language-image learning. In *CVPR*, pages 2818–2829, 2023. [5](#)
- [10] Wei-Lin Chiang, Zhuohan Li, Zi Lin, Ying Sheng, Zhanghao Wu, Hao Zhang, Lianmin Zheng, Siyuan Zhuang, Yonghao Zhuang, Joseph E. Gonzalez, Ion Stoica, and Eric P. Xing. Vicuna: An open-source chatbot impressing gpt-4 with 90%* chatgpt quality, 2023. [2](#)
- [11] Hyung Won Chung, Le Hou, Shayne Longpre, Barret Zoph, Yi Tay, William Fedus, Yunxuan Li, Xuezhi Wang, Mostafa Dehghani, Siddhartha Brahma, et al. Scaling instruction-finetuned language models. *arXiv preprint arXiv:2210.11416*, 2022. [2](#)
- [12] Wenliang Dai, Junnan Li, Dongxu Li, Anthony Meng Huat Tiong, Junqi Zhao, Weisheng Wang, Boyang Li, Pascale Fung, and Steven Hoi. Instructblip: Towards general-purpose vision-language models with instruction tuning. *arXiv preprint arXiv:2305.06500*, 2023. [1, 2, 3, 5](#)
- [13] Jia Deng, Wei Dong, Richard Socher, Li-Jia Li, Kai Li, and Li Fei-Fei. Imagenet: A large-scale hierarchical image database. In *CVPR*, pages 248–255. IEEE, 2009. [5, 6, 2](#)
- [14] Yinpeng Dong, Fangzhou Liao, Tianyu Pang, Hang Su, Jun Zhu, Xiaolin Hu, and Jianguo Li. Boosting adversarial attacks with momentum. In *CVPR*, pages 9185–9193, Salt Lake City, UT, USA, 2018. IEEE. [3](#)
- [15] Yinpeng Dong, Huanran Chen, Jiawei Chen, Zhengwei Fang, Xiao Yang, Yichi Zhang, Yu Tian, Hang Su, and Jun Zhu. How robust is google’s bard to adversarial image attacks? *arXiv preprint arXiv:2309.11751*, 2023. [1, 3](#)
- [16] Alexey Dosovitskiy, Lucas Beyer, Alexander Kolesnikov, Dirk Weissenborn, Xiaohua Zhai, Thomas Unterthiner, Mostafa Dehghani, Matthias Minderer, Georg Heigold, Sylvain Gelly, et al. An image is worth 16x16 words: Transformers for image recognition at scale. In *ICLR*, 2021. [2](#)
- [17] Yuxin Fang, Wen Wang, Binhui Xie, Quan Sun, Ledell Wu, Xinggang Wang, Tiejun Huang, Xinlong Wang, and Yue Cao. Eva: Exploring the limits of masked visual representation learning at scale. In *CVPR*, pages 19358–19369, 2023. [5](#)
- [18] Lianli Gao, Qilong Zhang, Jingkuan Song, Xianglong Liu, and Heng Tao Shen. Patch-wise attack for fooling deep neural network. In *ECCV*, pages 307–322. Springer, 2020. [3](#)
- [19] Ian J Goodfellow, Jonathon Shlens, and Christian Szegedy. Explaining and harnessing adversarial examples. In *ICLR*, pages 1–10, San Diego, CA, USA, 2015. <http://OpenReview.net>. [3](#)
- [20] Jindong Gu, Xiaojun Jia, Pau de Jorge, Wenqian Yu, Xinwei Liu, Avery Ma, Yuan Xun, Anjun Hu, Ashkan Khakzar, Zhijiang Li, et al. A survey on transferability of adversarial examples across deep neural networks. *arXiv preprint arXiv:2310.17626*, 2023. [3](#)
- [21] Andrew Ilyas, Logan Engstrom, Anish Athalye, and Jessy Lin. Black-box adversarial attacks with limited queries and information. In *ICML*, pages 2137–2146, Stockholm SWEDEN, 2018. PMLR. [3](#)
- [22] Alexey Kurakin, Ian Goodfellow, and Samy Bengio. Adversarial machine learning at scale. In *ICLR*, pages 1–17, Toulon, France, 2017. <http://OpenReview.net>. [3](#)
- [23] Chao Li, Shangqian Gao, Cheng Deng, De Xie, and Wei Liu. Cross-modal learning with adversarial samples. In *NeurIPS*, 2019. [3](#)
- [24] Junnan Li, Ramprasaath Selvaraju, Akhilesh Gotmare, Shafiq Joty, Caiming Xiong, and Steven Chu Hong Hoi. Align before fuse: Vision and language representation learning with momentum distillation. In *NeurIPS*, pages 9694–9705, 2021. [5](#)
- [25] Junnan Li, Dongxu Li, Silvio Savarese, and Steven Hoi. Blip-2: Bootstrapping language-image pre-training with frozen image encoders and large language models. In *ICML*, 2023. [1, 2, 3, 4, 5](#)
- [26] Aishan Liu, Tairan Huang, Xianglong Liu, Yitao Xu, Yuqing Ma, Xinyun Chen, Stephen J Maybank, and Dacheng Tao. Spatiotemporal attacks for embodied agents. In *ECCV*, pages 122–138. Springer, 2020. [3](#)
- [27] Haotian Liu, Chunyuan Li, Qingyang Wu, and Yong Jae Lee. Visual instruction tuning. In *NeurIPS*, 2023. [1, 2, 3, 5, 6](#)
- [28] Yanpei Liu, Xinyun Chen, Chang Liu, and Dawn Song. Delving into transferable adversarial examples and black-box attacks. In *ICLR*, 2017. [3](#)

- [29] Dong Lu, Zhiqiang Wang, Teng Wang, Weili Guan, Hongchang Gao, and Feng Zheng. Set-level guidance attack: Boosting adversarial transferability of vision-language pre-training models. In *ICCV*, pages 102–111, 2023. 3
- [30] Aleksander Madry, Aleksandar Makelov, Ludwig Schmidt, Dimitris Tsipras, and Adrian Vladu. Towards deep learning models resistant to adversarial attacks. In *ICLR*, pages 1–28, Vancouver, BC, Canada, 2017. <http://OpenReview.net>. 3, 5, 8
- [31] OpenAI. ChatGPT. <https://openai.com/blog/chatgpt>, 2022. 2
- [32] OpenAI. Gpt-4 technical report. *arXiv preprint arXiv:2303.08774*, 2023. 1, 2, 4
- [33] Nicolas Papernot, Patrick McDaniel, Ian Goodfellow, Somesh Jha, Z Berkay Celik, and Ananthram Swami. Practical black-box attacks against machine learning. In *ACM on Asia Conference on Computer and Communications Security*, pages 506–519, New York, NY, USA, 2017. Association for Computing Machinery. 3
- [34] Alec Radford, Jong Wook Kim, Chris Hallacy, Aditya Ramesh, Gabriel Goh, Sandhini Agarwal, Girish Sastry, Amanda Askell, Pamela Mishkin, Jack Clark, et al. Learning transferable visual models from natural language supervision. In *ICML*, pages 8748–8763. PMLR, 2021. 5, 6, 2
- [35] Robin Rombach, Andreas Blattmann, Dominik Lorenz, Patrick Esser, and Björn Ommer. High-resolution image synthesis with latent diffusion models. In *CVPR*, pages 10684–10695, 2022. 1, 4
- [36] Erfan Shayegani and Yue Dong. Jailbreak in pieces: Compositional adversarial attacks on multi-modal language models, 2023. 1, 3
- [37] Christian Szegedy, Wojciech Zaremba, Ilya Sutskever, Joan Bruna, Dumitru Erhan, Ian Goodfellow, and Rob Fergus. Intriguing properties of neural networks. In *ICLR*, pages 1–10, Banff, AB, Canada, 2014. <http://OpenReview.net>. 2
- [38] Ruixue Tang, Chao Ma, Wei Emma Zhang, Qi Wu, and Xiaokang Yang. Semantic equivalent adversarial data augmentation for visual question answering. In *ECCV*, pages 437–453. Springer, 2020. 3
- [39] Youze Wang, Wenbo Hu, Yinpeng Dong, and Richang Hong. Exploring transferability of multimodal adversarial samples for vision-language pre-training models with contrastive learning. *arXiv preprint arXiv:2308.12636*, 2023. 3
- [40] Xiaojun Xu, Xinyun Chen, Chang Liu, Anna Rohrbach, Trevor Darrell, and Dawn Song. Fooling vision and language models despite localization and attention mechanism. In *CVPR*, pages 4951–4961, 2018.
- [41] Lu Yu and Verena Rieser. Adversarial textual robustness on visual dialog. In *ACL*, pages 3422–3438, 2023. 3
- [42] Xiaohua Zhai, Alexander Kolesnikov, Neil Houlsby, and Lucas Beyer. Scaling vision transformers. In *CVPR*, pages 12104–12113, 2022. 5
- [43] Jiaming Zhang, Qi Yi, and Jitao Sang. Towards adversarial attack on vision-language pre-training models. In *ACM MM*, pages 5005–5013, 2022. 3
- [44] Richard Zhang, Phillip Isola, Alexei A Efros, Eli Shechtman, and Oliver Wang. The unreasonable effectiveness of deep features as a perceptual metric. In *CVPR*, 2018. 8
- [45] Susan Zhang, Stephen Roller, Naman Goyal, Mikel Artetxe, Moya Chen, Shuohui Chen, Christopher Dewan, Mona Diab, Xian Li, Xi Victoria Lin, et al. Opt: Open pre-trained transformer language models. *arXiv preprint arXiv:2205.01068*, 2022. 2
- [46] Yunqing Zhao, Tianyu Pang, Chao Du, Xiao Yang, Chongxuan Li, Ngai-Man Cheung, and Min Lin. On evaluating adversarial robustness of large vision-language models. In *NeurIPS*, 2023. 1, 2, 3, 5, 6
- [47] Ziqi Zhou, Shengshan Hu, Minghui Li, Hangtao Zhang, Yechao Zhang, and Hai Jin. Advclip: Downstream-agnostic adversarial examples in multimodal contrastive learning. In *ACM MM*, pages 6311–6320, 2023. 3
- [48] Deyao Zhu, Jun Chen, Xiaoqian Shen, Xiang Li, and Mohamed Elhoseiny. Minigt-4: Enhancing vision-language understanding with advanced large language models. *arXiv preprint arXiv:2304.10592*, 2023. 1, 2, 3, 5

INSTRUCTTA: Instruction-Tuned Targeted Attack for Large Vision-Language Models

Supplementary Material

6. Attack Cases

Fig. 6 shows an example to attack BLIP-2 for different methods. It can be seen from the figure that CLIP-based MF-it and MF-ii shows no targeted attack effect since they have the similar results with the clean sample. Interestingly, half of the response (*i.e.*, “a man and a woman”) of the adversarial sample generated by MF-it (EVA-CLIP) matches the original image and half (*i.e.*, “elephants in a zoo”) matches the target image. MF-ii (EVA-CLIP), InstructTA-MF-it and InstructTA-MF-ii demonstrate the targeted attack effect. Importantly, the description of our InstructTA-MF-ii best matches the target image.

7. Results with Complex Reasoning Questions

Inferring from images can demonstrate the model’s deep understanding of the image semantics. The box below shows some reasoning instructions from complex_reasoning_77k in LLaVA-Instruct-150K [27].

1. How can pedestrians ensure their safety when navigating this busy city scene at night?
2. What might the cat be curious about on the floor?
3. What suggestions can be made for individuals wishing to serve these dough balls in an aesthetically pleasing manner?
4. What might be the man’s intention in the kitchen?
5. How does the position of the players on the field affect their performance?
6. What unique feature can be observed about the desserts in the scene?
7. What type of event might be taking place in this scene?
8. What could be a possible reason for the dog and cat’s interaction?
9. In terms of architectural features, why might this clock tower be studied or admired?
10. What tactic might the man be employing during the tennis match?
11. What could be the significance or purpose of a single pink rose placed in a glass with water?
12. What can you infer about the laptop owner’s personal style or interests?
13. How is the truck being used during this event, and what challenges might it face in this context?
14. Why might the vandalized stop sign on the school bus cause concern?

...

To further evaluate the effectiveness of the proposed methods, we provide transfer attack results for complex reasoning instructions, as portrayed in Table 6. All methods, even clean samples, have obvious targeted attack performance. This may be because some of the selected reasoning instructions can be answered without the need for image information, *e.g.*, “Why might the vandalized stop sign on the school bus cause concern?”. Importantly, our methods have better transfer attack performances in terms of both CLIP score and the No. of successes. It implies that INSTRUCTTA still performs well even when faced with complex inference prompts.

8. Victim Models

Table 5 shows the architectures of the target LVLMs.

Table 5. The architectures of the victim LVLMs.

LVLM	Visual Encoder	Projector	LLM
BLIP-2	ViT-G/14 from EVA-CLIP	Q-Former & Single linear layer	Flan-T5-XXL
InstructBLIP	ViT-G/14 from EVA-CLIP	Q-Former & Single linear layer	Vicuna-7b-v1.1
MiniGPT-4	ViT-G/14 from EVA-CLIP	Q-Former & Single linear layer	Vicuna-v0-13b

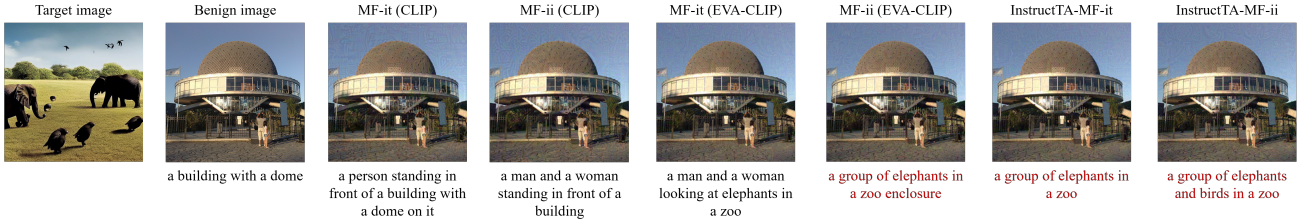


Figure 6. An instance of different targeted attack methods on BLIP-2. The real instruction is “Can you describe the main features of this image for me?”. The target text is “The image depicts a large elephant and a smaller elephant standing in a grassy area next to a stone wall, likely within a zoo enclosure. The two elephants appear to be gathered near a flock of black birds. The birds can be seen scattered around the enclosure, with some standing near the elephants and others in the background. The scene captures the interaction between the elephants and the birds, creating a serene and captivating moment.”

Table 6. **Targeted attacks against victim BLIP-2 with reasoning instructions.** We randomly select a total of 1,000 clean images from the ImageNet-1K [13] validation set. For each of these benign sample, a target text and a prompt are randomly assigned from complex_reasoning_77k in LLaVA-Instruct-150K [27]. Our metrics involves the computation of the CLIP score (\uparrow) [34, 46] between the target texts and the generated responses of AEs on the attacked LVM, which was performed using several CLIP text encoders and their ensemble. We also report the No. of successful attacks within 1,000 adversarial samples, determined by GPT-4. CLIP and EVA-CLIP in parentheses indicate that they are used as surrogate models for transfer attack.

VLVM	Attack method	Text encoder (pretrained) for evaluation						The No. of successes
		RN50	RN101	ViT-B/16	ViT-B/32	ViT-L/14	Ensemble	
BLIP-2	Clean image	0.609	0.662	0.646	0.651	0.506	0.615	381
	MF-it (CLIP) [46]	0.606	0.658	0.643	0.648	0.503	0.612	370
	MF-ii (CLIP) [46]	0.606	0.658	0.642	0.648	0.502	0.611	377
	MF-it (EVA-CLIP)	0.650	0.698	0.684	0.689	0.554	0.655	547
	MF-ii (EVA-CLIP)	0.646	0.696	0.679	0.685	0.545	0.650	529
	INSTRUCTTA-MF-it (ours)	0.650	0.699	0.683	0.689	0.551	0.654	566
	INSTRUCTTA-MF-ii (ours)	0.652	0.699	0.685	0.692	0.552	0.656	571